Final Report: Application of electron beam technology to decompose persistent emerging drinking water contaminants: poly- and perfluoroalkyl substances (PFAS) and 1,4-Dioxane

Award #DE-SC0020277

PI: Arjun K. Venkatesan**,** New York State Center for Clean Water Technology, Stony Brook University, Stony Brook, NY 11794

Co-PIs:
Charles Cooper, Fermi National Accelerator Lab. (FNAL), Batavia, IL, 60510
Doug Paquette, Brookhaven National Laboratory, Upton, NY
Marc A. Mills, US Environmental Protection Agency, Office of Research and Development, Cincinnati, OH

Researchers:
Kaushik Londhe, PhD Student, Stony Brook University
Cheng-Shiuan Lee, Research Scientist, Stony Brook University
Slavica Grdanovska, Associate Scientist, Fermi National Accelerator Lab

Summary

Poly- and perfluoroalkyl substances (PFAS) and 1,4-dioxane are persistent emerging contaminants that are currently under consideration for federal and state-specific regulations in drinking water. Both PFAS and 1,4-dioxane are highly resistant to degradation and are not effectively removed by conventional drinking water treatment systems. Results from the Unregulated Contaminant Monitoring Rule 3 survey showed that >540 sites across the nation are contaminated with both PFAS and 1,4-dioxane. Hence, there is a need to identify technologies that can effectively remove both these contaminants. Water treatment via electron beam (e-beam) has been proven effective at treating a wide range of contaminants, including perfluorooctane sulfonate (PFOS), perfluorooctanoate (PFOA), polychlorinated biphenyls, and trichloroethylene. While the e-beam process is often considered similar to advanced oxidation processes (AOPs), e-beam technology is unique in that it produces both highly oxidizing and reducing species at the same time. The specific objectives of this study were to: (i) determine the effectiveness of 9 MeV electrons provided by the Fermilab's Accelerator Application Development and Demonstration (A2D2) tool to decompose PFAS and 1,4-dioxane; (ii) assess the formation of byproducts during water treatment; (iii) apply the optimized treatment to field groundwater samples contaminated with PFAS and 1,4-dioxane, and (iv) assess the energy demands for the treatment of these contaminants using e-beam.

Results from this study showed that e-beam is effective in treating both 1,4-dioxane and PFAS. Complete degradation of 1,4-dioxane was observed at a dose of 5 kGy for an initial concentration of up to 1 ppm without the need for any sample modification. The electrical energy per order (EEo) for treatment of 1,4-dioxane ranged from 0.46 to 0.72 kWh/m^3/order and was comparable and even lower, in some cases, than other AOP technologies. Alkaline conditions (pH

13) and low dissolved oxygen concentration (2 mg/L) highly favored the treatment of PFAS by e-beam. Greater than 90% removal of PFOA and PFOS from an initial concentration of 100 to 500 ppb was achieved at a dose of 250 kGy and 500 kGy, respectively, under optimized conditions. The degradation efficiency was not significantly changed when treating other PFAS of fluorinated carbon chain length of 5 to 7 individually at 250 kGy with a removal ranging from 85–99% for different compounds. Short chain PFAS (perfluorobutanoate: PFBA and perfluorobutane sulfonate: PFBS) did not degrade under the same conditions at 250 kGy, but 70 to 99% degradation was observed at a higher dose of 1000 kGy.

Short chain PFAS (perfluorohexanoate: PFHxA (C5) and perfluoroheptanoate: PFHpA (C6)) were detected after treatment of PFOA, but not after PFOS treatment. Inability to close the mass balance through targeted analysis suggests the presence of other intermediates not detectable by available analytical methods. When treating PFAS mixture containing ten compounds at equimolar concentration of 0.05 μM each, preferential degradation of polyfluorinated compound (6:2 fluorotelomer sulfonate or 6:2 FTS) followed by C8 and C7 compounds was observed as a function of increasing e-beam dose. About 30% degradation of ΣPFAS was observed at 250 kGy and no further removal was observed up to a dose of 1000 kGy. C4 to C6 PFASs showed no degradation, while C3 PFAS (PFBS) showed an increase in concentration by 34% at 1000 kGy due to formation from the breakdown of other long chain PFAS. These results suggested that (a) the reaction kinetics is likely different for different PFAS based on chain length, functional group, and the degree of fluorination of the carbon chain, and (b) there may be intermediates generated from the degradation of 6:2 FTS and C7/C8 compounds that can potentially scavenge hydrated electrons needed for reaction with the untreated PFAS molecules. Treatment of three PFAS-contaminated groundwater samples from two US states showed similar trends as observed in the treatment of equimolar PFAS mixtures. Up to 71% removal of ΣPFAS was achieved in real groundwater samples at 750 kGy and data trend suggested that higher degradation is feasible if higher doses (>1MGy) are applied to treat field samples to overcome matrix effects and competing species. Calculated EEo for PFAS ranged from as low as ~48 to 1081 kWh/m^3/order depending on the type of PFAS treated. These values are comparable and even lower, in some cases, than other destructive technologies employed for PFAS treatment such as ultrasound, plasma, and photochemical treatment. The results from this study indicate e-beam is a promising approach under favorable conditions and should be explored further as an end-of-train treatment option for PFAS destruction.

1. INTRODUCTION

The ubiquitous use of per- and polyfluoroalkyl substances (PFAS) poses a grave challenge for water treatment. PFAS are anthropogenic chemicals that possess unique physical and chemical properties such as high thermal and chemical stability, low vapor pressure and surfactant-like properties[1-3]. These properties can be attributed to the PFAS structure where the hydrogens in an alkyl chain have been either partially (polyfluoro) or fully (perfluoro) replaced by fluorine atoms. PFAS have been extensively used in household and industrial applications such as firefighting foams, stain repellants, coatings, food packaging, and pesticide formations, masking tape as well as in patented brands such as ScotchGard and Teflon[1-4]. Due to their ubiquitous use, extreme thermal and chemical stability, and their resistance to natural and conventional water treatment systems, PFAS have been detected in various environmental compartments such as water, ice, landfills, soil etc. across the globe[1-3, 5-12]. The USEPA'S Third Unregulated Contaminant Monitoring Rule (UCMR3) study revealed the widespread contamination of PFAS in water throughout the U.S.[13].

1,4-Dioxane is another contaminant of emerging concern that was included by the USEPA on its initial list if 10 "high priority" chemical substances to be evaluated for human health risks. This was done as a part of 2016 amendments to the Toxic Substances Control Act. 1,4-Dioxane has also been classified as "a likely carcinogen" by USEPA, with drinking water being the potential exposure pathway[14, 15]. 1,4-Dioxane occurs in industrial waste streams due to its ubiquitous use as a solvent, stabilizing agent and can also be a byproduct of polyester manufacture[16]. It possesses high solubility in water and is also resistant to biodegradation and natural attenuation processes due to a low sorption and non-volatility[16]. The UCMR3 data found that 1,4-dioxane was detected at over 4000 sites across the U.S., with >600 sites having levels more than 0.35 μg/L, the level representing one-in-a-million cancer risk for people who drink it for a lifetime. Similar to PFAS, no federal maximum contaminant limit (MCL) currently exists for 1,4-dioxane.

Conventional water treatment techniques such as granular activated carbon (GAC) and anion exchange resins (AIX) have been used to remove PFAS from water with varied removal efficiencies. GACs have shown a range of 40-100% in removing short- and long-chain PFAS[1, 2, 17, 18], whereas techniques such as reverse osmosis (RO) and nanofiltration (NF) have been 50-100% effective in removing PFAS[2, 19, 20]. The variation in removal efficiencies is due to the wide variation in characteristics such as molecular weight, chain length, functional group of the PFAS studied, and as a result of water matrix effects. However, most of these approaches are considered as 'phase separation' techniques[6] that rely on merely removing PFAS from the water matrix. This results in a residual waste stream or sludge containing concentrated levels of PFAS that requires further treatment and disposal. On the other hand, 1,4-dioxane is not removed by phase separation techniques due to its low sorption coefficient and small molecule size[21]. Advanced oxidation processes (AOPs) that rely on the generation of hydroxyl radicals are capable of degrading 1,4-dioxane. However, AOPs are not effective in the treatment of PFAS. PFAS and 1,4-dioxane are examples of recalcitrant chemicals featuring completely different physicochemical properties making it difficult to identify one technology that can treat them all. Destructive techniques that can treat both PFAS and 1,4-dioxane by breaking down the molecules into less toxic and biodegradable products are needed as to solve contamination problems[1, 2, 6].

Electron beam (e-beam) is one of such destructive technique that utilizes ionizing radiation to breakdown recalcitrant chemicals[22, 23]. Unlike other destructive techniques that generate either oxidizing or reducing radicals, e-beam technology is unique in that it generates both oxidizing and reducing radical species after irradiation of water[22]. Irradiation of aqueous solutions with e-beam results in the decomposition of water molecules or water radiolysis that leads to the formation of various reactive species (radiolysis products of water) with the greatest number of protons (H^+), hydroxyl radicals ($OH^{\cdot}$), hydrated electrons (e_{aq}^-) produced as compared to other reactive species [22]. Amongst these species, hydrated electrons (e_{aq}^-) possess high reactivity and redox potential of -2.9 eV, making them suitable for degrading PFAS[1, 24-26]. The hydroxyl radicals ($OH^{\cdot}$) simultaneously generated can react and degrade 1,4-dioxane molecules[14, 27].

There are a limited number of studies (n = 7) that have utilized e-beam technology to study PFAS degradation[1, 26, 28-30]. These studies have focused on either degradation of solely PFOA or PFOS while some of them have compared their degradation in mostly drinking water but also wastewater matrices[26, 28-32]. Researchers have primarily relied on AOPs for the degradation of 1,4-dioxane and not utilized high energy e-beam to study its degradation. In this project we utilized e-beam technology to treat a suite of PFAS and 1,4-dioxane and assessed the effects of various operating and water quality parameters on treatment efficiency. The main objectives of the project are to:

- determine the effectiveness of 9 MeV electrons provided by the Fermilab's Accelerator Application Development and Demonstration (A2D2) tool to decompose PFAS and 1,4-dioxane,
- test the impacts of additives and other water quality parameters on the performance of e-beam to remove contaminants,
- evaluate the formation of byproducts resulting from PFAS and 1,4-dioxane degradation using e-beam,
- evaluate the effectiveness of e-beam technology to degrade environmentally relevant levels of PFAS and 1,4-dioxane in contaminated groundwater samples, and
- estimate the energy demands associated with e-beam treatment of PFAS and 1,4-dioxane.

2. MATERIALS AND METHODS

2.1. Sample preparation.

All chemicals and solvents used in this research were of either certified ACS reagent grade or LC/MS and GC/MS grade with high purity and were purchased from Sigma-Aldrich and Fisher Scientific. Samples were prepared by Stony Brook University in borosilicate glass or polypropylene vials obtained from Fisher Scientific. Empty weight of the vials was noted before sample preparation. Three separate 1 L polypropylene jars were used to prepare deionized water (DIW) with the pH adjusted to 4, 10 or 13 as per necessary. The pH was adjusted by adding NaOH (for pH 10, 13 samples) or by using HCl, H_2SO_4, or HNO_3 for pH 4 samples. 15 mL or 160 mL of DIW was transferred into individual containers and the samples were spiked using stock solutions of PFAS (10 ppm) and/or 1,4-dioxane. Four samples were prepared for each sample set conditions. Three samples in the set were shipped to Fermilab for treatment and one sample was retained to measure initial concentration of the contaminant prior to treatment. In each batch, control samples with known concentration of the contaminants and a sample containing only DIW (no additives and no contaminants) were simultaneously prepared and shipped to Fermilab. These samples were not treated but accounted for any loss in concentration and external contamination during sample

processing. Samples were weighed post preparation to verify the volume and were sealed using a tape. Samples were placed in Styrofoam holders and were shipped overnight to Fermi National Accelerator lab for treatment.

2.2. E-beam treatment.

Fermilab houses a demonstration accelerator (Accelerator Application Development and Demonstration, A2D2) that enables proof-of-concept studies. A2D2 is a 9 MeV electron accelerator and is provided by a repurposed teletherapy linac. It is a normal conducting multi-cell 2.85 GHz accelerator structure. Electrons are generated by a thermionic electron gun and is powered by a classic Klystron amplifier. Once the electrons are accelerated, they are collimated by thin slits and a 270-degree bending magnet. When combined, these electrons have a narrow momentum spread and are well focused leaving the vacuum window. With variable settings the machine can provide a maximum of 1.2 kW of beam power and electron kinetic energy of 9 MeV.

Dosimetry is provided by a NIST certified dosimetry system that is available to measure/verify the amount of total dose given to each sample. For all samples to be placed in the electron beam, an optical density film is placed alongside the sample. The dosimetry method used to measure absorbed dose for e-beam irradiations is Far West Film dosimetry (FWT-60, Far West Technology, Inc., Goleta, CA). These 44.5 μm thin radiachromic films are derivatives of the family of aminotriphenyl-methane dyes that gradually change from colorless to a deeply colored state as a function of absorbed dose. Specifically, these dosimeters use a hexa(hydroxyethyl) aminotriphenylacetonitrile (HHEVC) dye. Their absorbed radiation dose range is 0.5 to 200 kGy and they are measured by observing the color change at a wavelength of 510 nm or 600 nm by photometer or spectrophotometer. A major advantage to these nylon-based thin films is their "tissue-equivalence", meaning the response of the film is equivalent to that of tissue, water and many polymers with a density ~ 1 g/cm^3. This means that the dose received by the film can be considered approximate to the dose received by the sample with comparable density.

A summary of various treatment conditions tested in this project is provided in Table 1. The samples were treated as batch systems using the 9 MeV electron beam located at Fermilab. Upon receiving the samples at Fermilab, samples were purged with high purity N_2 gas to attain a final dissolved oxygen (DO) concentration of 2 mg/L for PFAS treatment. Samples were treated in sealed containers as received for 1,4-dioxane. The dose rate was fixed at 1.2 kGy/sec and the e-beam irradiation time determined the applied dose. The sample depth in each of the container was carefully chosen to match the penetration depth of the e-beam (3 cm). To maximize usefulness of A2D2 beam time, samples were treated in set of six for each irradiation. For dose uniformity, the samples were placed in revolving hexagonal shaped sample holder. After sample treatment, the samples were sealed and were shipped on ice back to Stony Brook University for analysis.

2.3. Analysis of PFAS and 1,4-dioxane.

Upon receiving the samples at Stony Brook University, samples were weighed to account for any loss in sample volume during sample shipment and processing. Samples were diluted (1:1) with methanol to prevent any sorption prior to PFAS analysis. An aliquot of samples was taken out for further dilution (to fall within the calibration) and the pH was adjusted to near neutral using 10 % acetic acid. Samples were analyzed for PFAS using an Agilent 6495B triple quadrupole liquid chromatography tandem mass spectrometer (LC-MS/MS) equipped with electron spray ionization (ESI) available at Stony Brook University (Appendix). Samples containing 1,4-dioxane

were extracted by liquid-liquid extraction and analyzed using an Agilent 7890/5975 gas chromatography mass spectrometer (GC/MS) (Appendix).

Table 1: Summary of treatment conditions tested for PFAS and 1,4-dioxane.

Parameter Studied	Contaminant(s)	Value Range
pH	PFAS, 1,4-dioxane	pH 4, 10 ,13
Initial concentration	PFAS	100, 500 ppb
	1,4-dioxane	100 ppb – 1000 ppm
Dissolved oxygen (DO)	PFAS, 1,4-dioxane	2 mg/L – 8.5 mg/L
E-beam dose	PFAS	25 – 1000 kGy
	1,4-dioxane	2.5 – 25 kGy
Co-contaminants	PFAS mixture	-
	PFOS, PFOA, 1,4-dioxane	
Groundwater matrix	PFAS mix, 1,4-dioxane	

3. RESULTS AND DISCUSSION

3.1. Optimization of sample volume and container material.

Preliminary experiments were conducted to test the feasibility of using e-beam to treat PFAS and 1,4-dioxane. PFOS and PFOA were used as model contaminants to optimize treatment conditions.

Sample container: Three different container material was tested to assess its interaction with the contaminants and treatment efficiency: borosilicate glass, soda lime glass, and polypropylene jars. Borosilicate glass worked ideally for both PFAS and 1,4-dioxane. Soda lime glass container became fragile after irradiation and hence was not used further. We did not observe any significant loss of contaminants in our control jars due to adsorption for a period of 14 days. Polypropylene worked well for PFAS, but the container was not ideal for 1,4-dioxane treatment as it eluted organic byproducts after e-beam irradiation that interfered with byproduct assessment. Hence borosilicate and polypropylene containers were used for PFAS alone treatments, whereas glass jars were used for 1,4-dioxane treatment.

Sample volume: Four different sample volumes were treated depending on the dimensions of the jars: 15 mL, 90 mL, 130 mL, and 160 mL. The goal was to maintain a constant sample depth of 3 cm to match the penetration depth of the electron beam radiation. Results revealed that the treatment efficiency for both PFAS and 1,4-dioxane did not vary between different sample volumes, confirming that the depth of the water was the determining factor for treatment as long as the irradiation is uniform throughout the cross section of the sample container.

3.2. Derivation of Electrical Energy per Order (EEo) equation for e-beam applications.

Electrical energy per order (EEo) can be defined as the energy required for one log removal (90% removal) of a contaminant in a unit volume of water. It is typically used to evaluate the energy efficiency of advanced oxidation processes (AOP) to degrade a target contaminant[14]. Here, we developed an equation for determining the EEo for e-beam treatment of water as follows. EEo for AOP systems can be calculated using the following equation[14]

$$\text{EEo (kWh m}^{-3}\text{ order}^{-1}) = \frac{P * t * 1000}{V * 60 * \log(\frac{[C]in}{[C]out})} \quad \text{- Equation 1}$$

Where, *P* is the power (kW), *t* is the time (min), *V* is the sample volume (L), C_{in} is the influent concentration and C_{out} is the effluent concentration of the target contaminant. For e-beam treatment of 'y' mL water sample receiving a dose of 'x' kGy by using unit conversion as follows[1]:

$$\text{EEo (kWh m}^{-3}\text{ order}^{-1}) = \frac{x\ kGy * \left(\frac{kJ}{kGy * kg} * \frac{kg}{1000\ ml} * y\ ml\right) * \frac{kWh}{3600\ kJ}}{y\ ml * \frac{1\ L}{1000\ ml} * \frac{1\ cu.m}{1000\ L} * \log(\frac{[C]in}{[C]out})} \quad \text{- Equation 2}$$

$$\text{EEo (kWh m}^{-3}\text{ order}^{-1}) \text{ for e-beam} = \frac{Dose\ (kGy)}{3.6 * \log(\frac{[C]in}{[C]out})} \quad \text{- Equation 3}$$

Where, *Dose* denotes the dose delivered to the water sample in unit of kGy (kJ kg^{-1} of water). Since, EEo is based on measurable variables and can be confirmed by measuring contaminant log reduction and dose applied, we can use the EEo values to compare between ecustring e-beam treatment technologies as well as other destructive technqiues such as advanced ocistaion processes, electrochemical oxidation, sonolysis, plasma treatment and sonolysis

3.3. Degradation of 1,4-dioxane by e-beam.

To the best of our knowledge, 1,4-dioxane has not been evaluated for treatment by e-beam. Our preliminary experiments revealed complete degradation of 1,4-dioxane when an initial concentration of 100 – 1000 ppb (µg/L) was treated using 5 – 50 kGy of e-beam dose in DIW. Complete degradation of 1,4-dioxane was observed even when 1000 ppb was treated at 5 kGy (Table 2). 5 kGy was the lowest and confident dose that the Fermilab could deliver using the accelerator at a dose rate of 1.2 kGy/sec. Complete degradation was observed irrespective of different pH (4–13) and DO concentrations (2–8.5 mg/L) of water samples. The solution pH can affect the abundance of reactive species such as e_{aq}^- and $OH^{\cdot}$, according to reactions 1 and 2[26]. $OH^{\cdot}$ radicals, primarily responsible for 1,4-dioxane degradation[14], can be scavenged by OH^- ions at higher pH conditions. However, we did not observe such an effect under the conditions tested for e-beam, suggesting high efficiency of hydroxyl radical production by water radiolysis by e-beam. These results suggested 1,4-dioxane can be treated without the need for any sample modification.

$$e_{aq}^- + H^+ \rightarrow H^{\cdot} \quad \text{- Reaction 1 } (k = 2.2 \times 10^{10}\ M^{-1}s^{-1})$$
$$OH^{\cdot} + OH^- \rightarrow O^{\cdot -} + H_2O \quad \text{- Reaction 2 } (k = 1.2 \times 10^{10}\ M^{-1}s^{-1})$$

Table 2. Degradation data for 1,4-dioxane using e-beam with varying initial concentrations and water quality parameters

pH	Dosage (kGy)	1,4-Dioxane Initial (ppb)	1,4-Dioxane post degradation (ppb)	EEo (kWh/m^3/order)
-	5	83	<1.0	0.72
-	5	410	<1.0	0.53
-	5	968	<1.0	0.46
4	5	1015	<1.0	0.46
8	5	991	<1.0	0.46
13	5	1012	<1.0	0.46

To generate 1,4-dioxane degradation kinetics, we increased the initial concentration to 1000 ppm (mg/L) and applied a dose of 10, 15, 20, and 25 kGy. The degradation showed a linear increase with increase in dose applied with a 38% degradation of 1,4-dioxane observed at the highest treatment dose of 25 kGy. It must be noted that the 1000 ppm is not environmentally relevant levels and is highly concentrated to generate degradation kinetics. The degradation followed pseudo-first order kinetics (Figure 1b) with a rate constant of 1.8 x 10^{-2} s^{-1} at a constant dose rate of 1 kGy/sec.

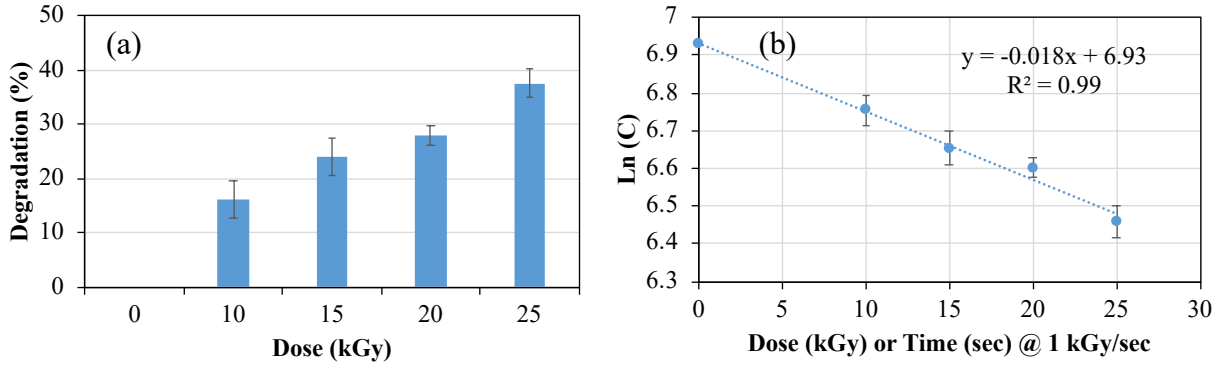

Figure 1. (a) Percent degradation of 1,4-dioxane with varying e-beam dose. Initial concentration:1000 ppm. Error bars represent standard deviation for triplicate samples. (b) First-order kinetic fit for 1,4-dioxane degradation.

Interestingly, at this high concentration we were able to observe the effect of DO concentration on 1,4-dioxane. Purging the samples to a lower DO level of 2 mg/L improved the degradation efficiency by ~22% compared to no purge samples (Figure 2). To the best of our knowledge, hydroxyl radicals in solutions are not consumed by dissolved oxygen. This observation may imply that other oxygen-sensitive reactive species generated by e-beam irradiation may assist with 1,4-dioxane degradation. Its underlying mechanism(s) needs further investigation. However, this improvement in degradation is minimal and might not justify the need for additional energy of purging when treating environmentally relevant levels (Table 2), where complete degradation was observed even at low treatment dose.

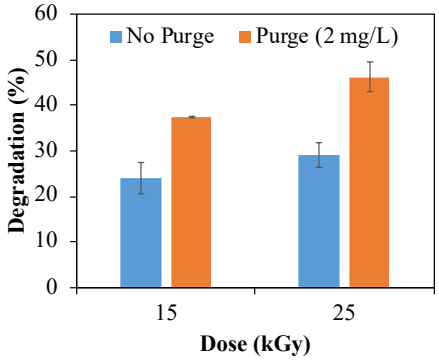

Figure 2. Effect of DO concentration on 1,4-dioxane degradation by e-beam. Error bars represent standard deviation for triplicate samples.

The calculated EEo, using equation 2, ranged from 0.46 – 0.72 kWh/m^3/order for 1,4-dioxane using e-beam. It must be noted that the detection limit of 1 ug/L was used as the treated concentration for determining the EEo values. Hence, these numbers are higher estimates than the actual EEo value. Previous studies have utilized e-beam to degrade persistent organic pollutants such as diclofenac, chlortetracycline, chloroform, bromoform Iopromide amongst others in different water matrices at neutral pH conditions. The calculated EEo values, based on the delivered e-beam dose ranged from 0.04 and 0.17 kWh/m^3/order for chlortetracycline and tetrachloroethylene respectively to 1.67 and 248.2 kWh/m^3/order for Iopromide and 2,3,7,8-PCDD/Fs respectively[1]. For 1,4-dioxane, the EEo values using advanced oxidation processes ranged from 0.13-7.4 kWh/m^3/order[14]. Thus, based on these calculated EEo values, e-beam technology is highly effective at degrading 1,4-dioxane.

3.3.1. Byproducts of 1,4-dioxane.

Aldehydes and organic acids are the primary byproducts of 1,4-dioxane oxidation by hydroxyl radicals[33, 34]. We detected formaldehyde, oxalate, acetate, and formate after treatment of 1,4-dioxane using e-beam (Figure 3). Oxalate was the most abundant byproduct, followed by acetate and formate. These levels are consistent with other AOP technologies treating 1,4-dioxane at 100 ppb[33]. It can also be observed that the concentration of byproducts increased with increasing initial concentration of 1,4-dioxane, except for formaldehyde. We did not observe any trend for formaldehyde formation. The concentration of organic acids reduced with increasing e-beam dose, suggesting that complete oxidation of 1,4-dioxane to CO_2 and H_2O is feasible at higher doses.

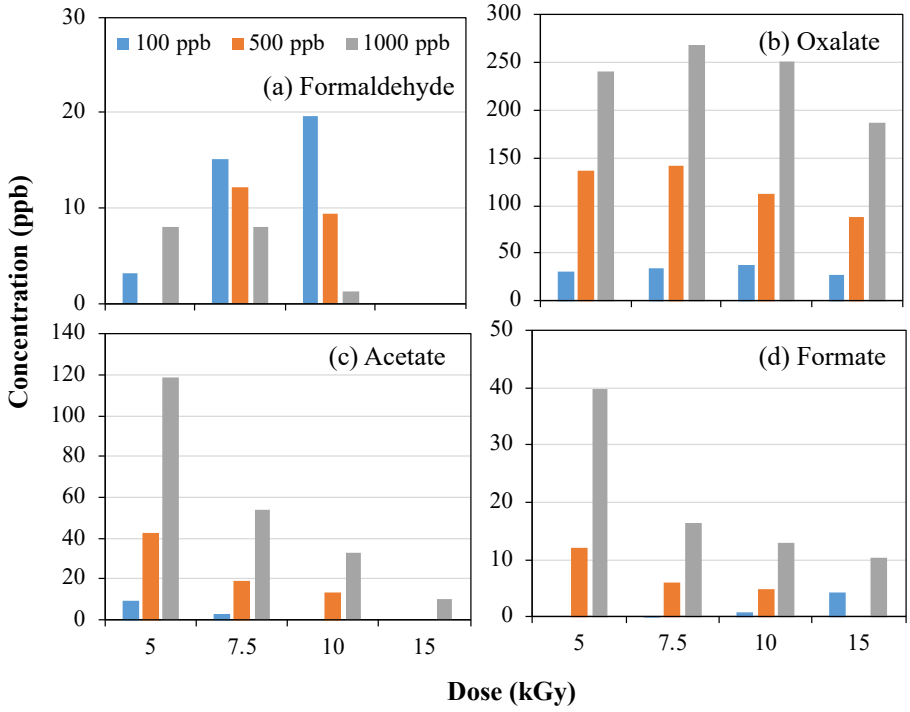

Figure 3. Degradation byproducts of 1,4-dioxane as a function of 1,4-dioxane initial concentration and e-beam dose.

3.4. Degradation of PFOS and PFOA by e-beam.

Previous studies have identified e_{aq}^- (E = -2.9 eV) as the primary reactive specie responsible for reacting with and breaking down the C-F bond in PFAS while utilizing e-beam[26, 28, 29, 31]. e_{aq}^-

can react with PFOA (Reaction 3) and PFOS (Reaction 4), forming PFAS radicals, that can further undergo decomposition.

$e_{aq}^- + C_7F_{15}COO^- \rightarrow C_7F_{15}COO^{\cdot 2-}$ - Reaction 3 ($k = 1.7 \times 10^7 M^{-1}s^{-1}$ - $7 \times 10^7 M^{-1}s^{-1}$)
$e_{aq}^- + C_8F_{17}SO_3^- \rightarrow C_8F_{17}SO_3^{\cdot 2-}$ - Reaction 4 ($k = 0.56 \times 10^7 M^{-1}s^{-1}$ - $7 \times 10^7 M^{-1}s^{-1}$)

e_{aq}^- however, can undergo scavenging by other reactive species such as $OH^{\cdot}$, H^+ and $H^{\cdot}$, leading to the reduction in e_{aq}^- available to react with PFAS molecules[35]. Moreover, water quality parameters such as dissolved oxygen[26, 28, 31] (DO) and pH[26, 31] can also impact the abundance of e_{aq}^-, according to reactions 1, 2, 5, and 6. Thus, sample pretreatment such as adjusting pH, purging gas, or adding additive is critical to maximizing the removal performance.

$e_{aq}^- + O_2 \rightarrow O_2^-$ - Reaction 5 ($k = 1.9 \times 10^{10} M^{-1}s^{-1}$)
$e_{aq}^- + OH^{\cdot} \rightarrow OH^-$ - Reaction 6 ($k = 3 \times 10^{10} M^{-1}s^{-1}$)

3.4.1. Effect of DO and sample pH on PFAS degradation

We tested the effect of DO concentration by purging nitrogen gas prior to treatment of PFOA and PFOS at an initial concentration of 100 ppb and an e-beam dose of 200 kGy. Two target DO concentrations of 4 mg/L and 2 mg/L were tested along with no purge condition. As shown in Figure 4, both PFOA and PFOS degradation improved with decreasing DO concentration with an improvement by 47% for PFOA and 23% for PFOS at 2 mg/L compared to no purge samples. Previous studies have also reported an improvement in the percent degradation as a result of purging with gases such as argon, air, or nitrogen[26, 28, 31, 32]. Reactions 1 and 5 depict the scavenging effect of DO and protons on e_{aq}^-. These reactions can reduce the availability of e_{aq}^- to react with and degrade PFAS in water matrix, thus negatively affecting the overall degradation.

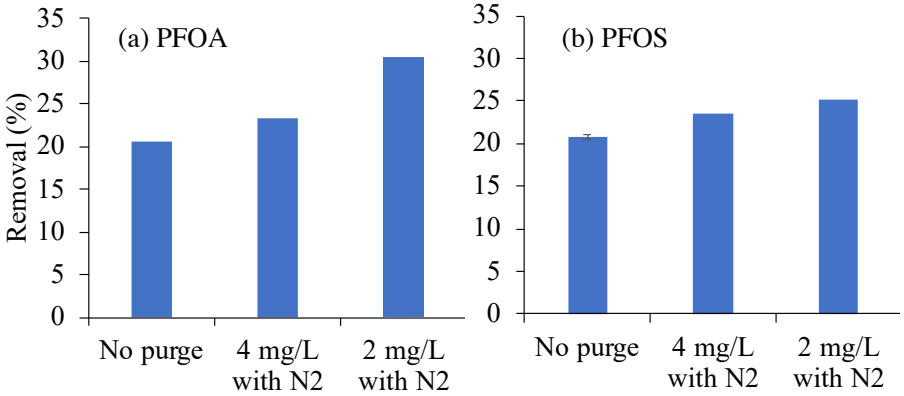

Figure 4. Effect of DO concentration on PFAS degradation.

The impact of pH on PFAS degradation at 2 mg/L DO concentration is summarized in Figure 5. pH 13 yielded the highest percent degradation for both PFOS (77 – 99%) and PFOA (92 – 99%) (Figure 5). Contrary to previous literature, there was no observable trend with an increase in pH from 4 to 13 for both PFOS and PFOA.

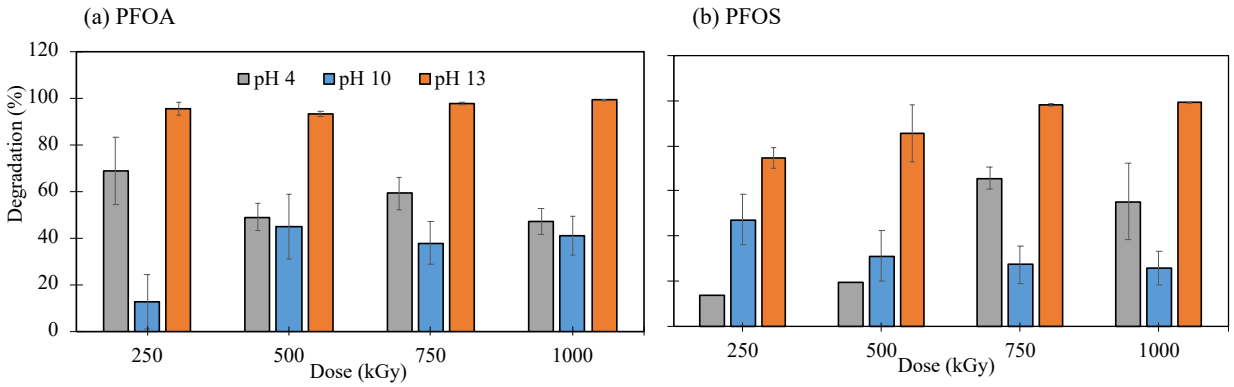

Figure 5. Percent degradation of a) PFOA and b) PFOS at different pH conditions as a function of e-beam dose. Initial concentration: 100 ppb. Error bars represent standard deviation for triplicate samples

The first-order rate constant for PFOS degradation at pH 13 was found to be k = 5 $\times 10^{-3}$ kGy^{-1} (s^{-1} at constant dose rate of 1 kGy/s) which was higher than the rate constants reported in previous studies[36] (1.038 –1.9 $\times 10^{-3}$ kGy^{-1}). At pH 13, there is lower H^+ ion concentration to react with and scavenge e_{aq}^- from the solution (Reaction 1). Although $OH^{\cdot}$ can also scavenge e_{aq}^-, at pH 13, their abundance is reduced due to reactions with OH^-, abundantly present at high pH, according to Reaction 2. Additionally, oxide radical anions generated at high pH (Reaction 2) can further react with dissolved oxygen (Reaction 7)[30], greatly eliminating this e_{aq}^- scavenger in the solution. As a result, these factors contribute to increasing the abundance of e_{aq}^- at pH 13, enabling more reactions with PFAS molecules compared to pH 4 and 10. Previous studies have also investigated the effect of pH on the overall treatment process. A study conducted in 2017[31] reported an increase in degradation efficiency with an increase in pH[31]. This was attributed to the lack of scavenging reactions (Reaction 6) with increasing pH that can reduce the abundance of $OH^{\cdot}$ radicals from the solution. As a result, we identified the ideal conditions for degradation of PFAS using the e-beam system as pH 13 by NaOH addition with 2 mg/L DO by N2 purging.

$$O^{\cdot -} + O_2 \rightarrow O_3^{\cdot -} \qquad \text{- Reaction 7 } (k = 3 \times 10^9\ M^{-1}s^{-1})$$

3.4.2. Effect of additives on PFAS degradation

In addition to studying the effect of pH, we also studied the impact of various acids to see if different anions played a role in the degradation of PFAS. For this purpose, the pH was adjusted to 4 by nitric acid, hydrochloric acid, and sulfuric acid in samples containing 100 ppb of PFOS and treated at a dose of 375 kGy (Figure 6). As seen in Figure 6, at pH 4, the three samples, with pH adjusted by different additives yielded similar percent degradation. This suggested that the anions did not play a role in the degradation mechanism of PFAS and that the pH (proton concentration) was more important. Previous studies have reported an improvement in the percent degradation of PFAS in the presence of nitrate ions[26, 32]. This was theorized to be due to the formation of nitrate radicals (E = −1.1 eV) and nitrogen dioxide radicals that can further react with and degrade PFOA from the solution[32]. However, we did not observe such effects in our experiments. The difference could be that we tested the treatment of PFOS and not PFOA like the previous study. We are unsure whether the functional group (sulfonate vs carboxylate) have different reactivity with nitrate radicals.

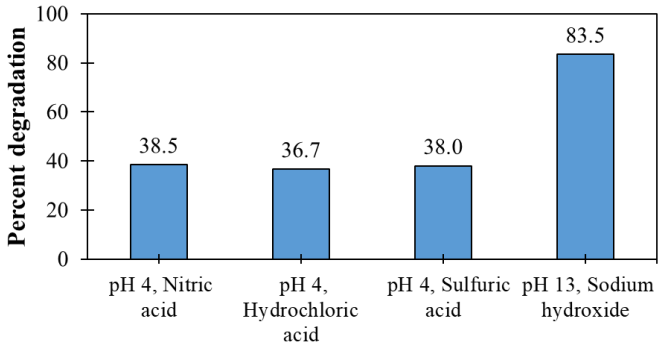

Figure 6. Percent degradation of PFOS with pH adjusted by different acids and base. Initial PFOS concentration: 100 ppb, DO: 2 mg/L, e-beam dose: 375 kGy.

3.4.3. Effect of initial concentration of PFOA and PFOS on degradation efficiency.

In order to observe the effect of initial concentration on the overall treatment of PFOS and PFOA, two concentrations (100 and 500 ppb) were treated with increasing e-beam dose. Samples were treated at pH 13 and were purged with N_2 to obtain a final DO concentration of 2 mg/L. As shown in Figure 7, the degradation of PFOS and PFOA was similar for both initial concentrations tested. PFOA showed >90 % degradation at a dose of 250 kGy and PFOS showed >90% degradation at a dose of 500 kGy. This finding suggests that the e-beam irradiation produces enough number of e_{aq}^- to react with PFAS molecules, but the percentage degradation is rather limited by the competition between PFAS molecules and other e_{aq}^- scavengers like H^+, $OH^\cdot$ etc. This can be explained by the fact that 90% removal of 100 ppb and 500 ppb initial concentration represent a reduction of 90 ppb and 450 ppb of PFAS after treatment. It is theorized that at higher initial concentrations, the relative abundance of PFAS molecules available to react with e_{aq}^- increases compared to other reactive species, thus helping to minimize the scavenging of e_{aq}^- by other species of water radiolysis[1]. This finding suggests that it would be more energy efficient to treat a concentrated PFAS solution while utilizing e-beam technology [1, 12]. Identifying the optimal initial concentrations and the required dose for a particular e-beam treatment setup would be vital to lower the overall EEo values of the process.

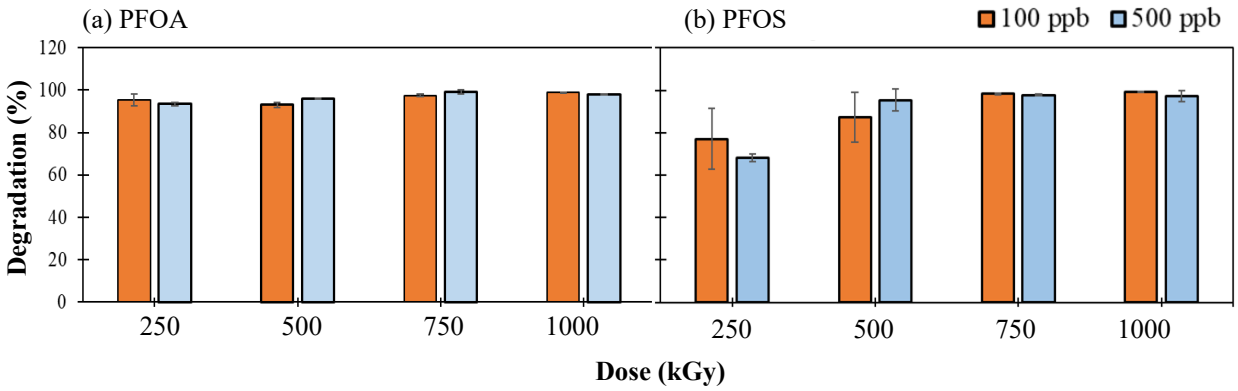

Figure 7. Degradation of PFOA and PFOS at different initial concentrations and varying e-beam doses. Error bars represent standard deviation from triplicate samples.

3.4.4. Byproducts of PFOS and PFOA degradation after e-beam treatment.

We measured a suite of PFAS compounds and inorganic fluoride after treatment of PFOS and PFOA to observe if short-chain PFAS compounds were generated to indicate reductive defluorination reactions. We did not detect fluoride ions (detection limit = 10 µg-F/L) due to matrix interference and high detection limit featured in our instrument. We did not detect any short-chain PFAS after PFOS treatment. However, short chain perfluoroalkyl carboxylates were detected after PFOA treatment. PFHxA and PFHpA were detected after treating 100 ppb for PFOA as shown in Figure 8. From Figure 5, it can be noted that the degradation of PFOA at pH 4 and pH 10 was less compared to pH 13. Interestingly the levels of PFHxA and PFHxS were higher in pH 4 and 10 compared to pH 13. This suggested that at pH 13, better transformation of PFOA could be achieved. However, without the measurement of total organic and inorganic fluoride in treated samples, we are unable to comment on the presence of other per- or polyfluorinated intermediates.

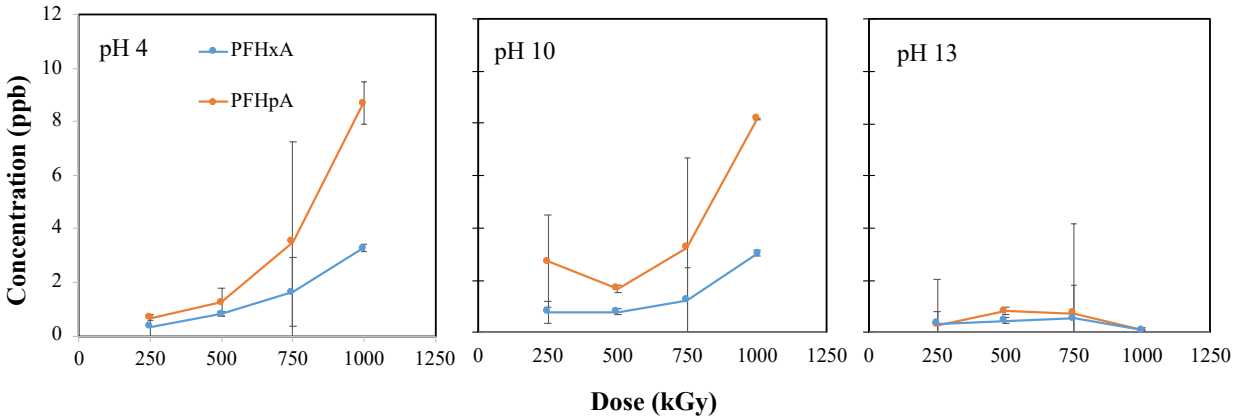

Figure 8. Generation of short chain PFCAs after treatment of PFOA as function of e-beam dose. Initial concentration of PFOA = 100 ppb. Error bars represent standard deviation from triplicates.

3.4.5. PFOS isomer degradation.

Linear and branched isomers of PFOS exist in the environment. The ration of linear-to-branched can vary significantly depending on the source of contamination and physical-chemical processes occurring in the environment. The branched form of PFOS can vary from <10 % to 75% of the total PFOS concentration in aquatic systems[37]. Hence it is important to understand the differences in treatment of PFOS isomers. Our analytical methods were able to differentiate between linear and branched form of PFOS. About 30% of the total PFOS is represented by branched isomers in our experiments. The percentage removal of branched and linear PFOS during e-beam treatment is summarized in Figure 9. As seen, for pH 4 – pH 13, branched isomers are easily degraded by e-beam compared to the linear form. The difference in degradation of PFOS as a function of pH is mainly due to the resistance to degradation by the linear isomer. Branched isomers show similar degradation profile irrespective of the solution pH. This can likely be due to higher reactivity of the branched isomer of PFOS with e_{aq}^- compared to the linear form. Preferential degradation of branched isomer of PFOS over the linear form has also been observed for other treatment technologies[30, 38].

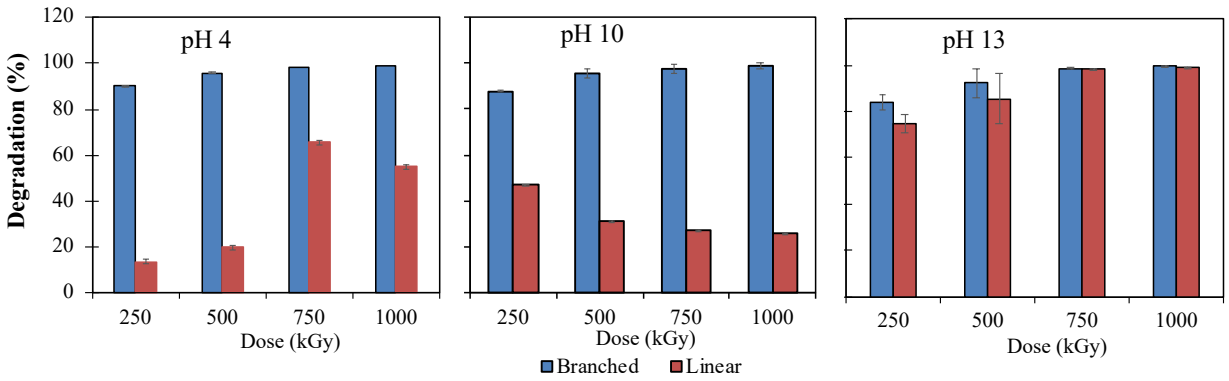

Figure 9. Degradation of branched vs. linear isomer of PFOS during e-beam treatment.

3.5. Impact of PFAS chain length, functional group on degradation efficiency.

Ten PFAS compounds of perfluorinated carbon chain length ranging from 3 to 8 were treated individually at 250 kGy and using the optimized pH and DO conditions. The compounds included six perfluoroalkyl carboxylates: PFCAs (PFBA, PFPeA, PFHxA, PFHpA, PFOA, PFNA), three perfluroalkyl sulfonates: PFSAs (PFBS, PFHxS, PFOS), and one fluorotelomer sulfonate (6:2 FTS). The degradation percentage observed with increasing chain length of the perfluorinated carbon is shown in Figure 10. It must be noted that the carbon associated with the carboxylate functional group is not considered in the perfluorinated chain length listed in Figure 10. It can be observed that the degradation efficiency was similar for compounds with same perfluorinated carbon chain length irrespective of the functional group, except for C4 compounds. We did not observe any degradation for PFBS (C4) under the tested conditions, but C4 PFCA (PFPeA) showed complete degradation. C3 PFCA (PFBA) showed negligible removal at 250 kGy (average 14% removal), similar to PFBS. These results suggest that the functional group might influence PFAS reactivity with e_{aq}^- when the chain length is shortened. More research is needed to understand the observed trend.

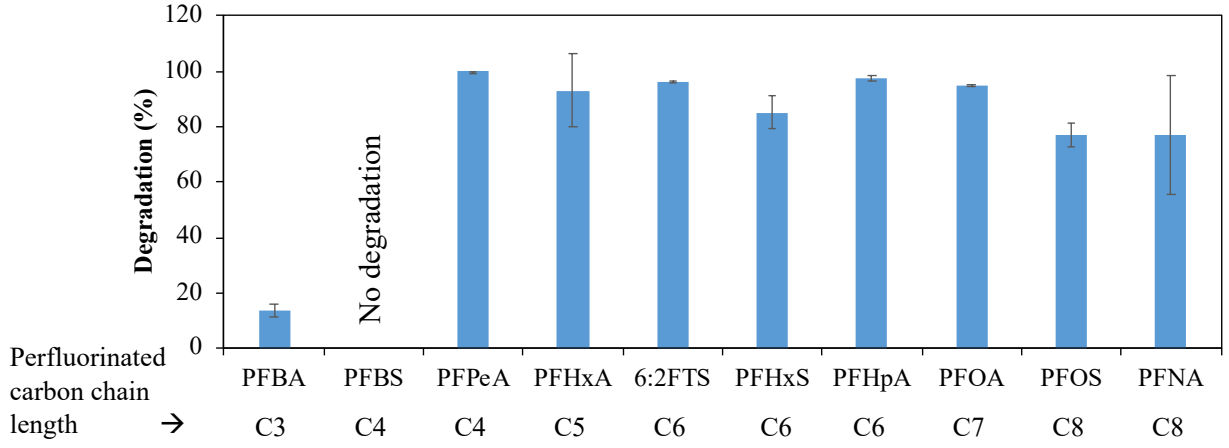

Figure 10. Percent degradation of PFCAs and PFSAs of different chain lengths and 6:2 FTS at a fixed dose of 250 kGy. Initial concentration of individual PFAS: 100 ppb, DO: 2 mg/L. Perfluorinated carbon chain length does not include the carbon in the carboxylate functional group.

The removal percentage observed for C5 to C7 PFASs were not significantly different and their average removal ranged from 85–97% at 250 kGy. 6:2 FTS showed 96% degradation although the total carbon chain length is 8 (six carbons are perfluorinated and 2 carbons are hydrogenated). This further confirms that the C-F bonds are the limiting factor for the degradation via reaction with e_{aq}^-. The average removal for C8 compounds (PFOS and PFNA) was slightly lower at 77% at 250 kGy compared to C5 to C7. PFBA and PFBS showed the least degree of degradation as compared to other PFAS under similar conditions at 250 kGy. This could be due to relatively higher stability of C-F bonds in short chain PFAS that result in resistance to degradation[39]. We treated PFBS and PFBA at 1000 kGy and we observed an average of 99% removal of PFBA and 72% removal of PFBS (Figure 11). This suggests that more reaction time and /or energy is required to breakdown these short-chain molecules. More research on the interactions of short chain PFAS with reactive species and a study of bond energy data for short chain PFAS is needed to better understand the degradation mechanisms and chain length dependence.

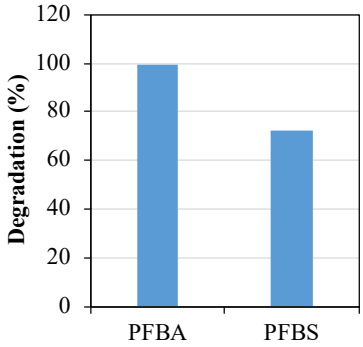

Figure 11. Degradation of PFBS and PFBA at 1000 kGy dose, pH 13, and 2 mg/L of DO.

3.5.1. Treatment of PFAS mixtures using e-beam.

AFFF-impacted waters usually feature a suite of PFAS compounds. As noted in the previous section, the reactivity of PFAS is chain length dependent and it is important to understand how PFAS mixtures would behave under e-beam irradiation. To assess competitive breakdown, we treated equimolar mixture of 10 PFAS mixture (0.05 μM each) at optimized treatment conditions from previous sections (pH 13, 2 mg/L DO) with varying e-beam doses ranging from 125 kGy to 1000 kGy. About 30% of total PFAS was degraded at 250 kGy, beyond which no further reduction in total PFAS concentration was observed (Figure 12a).

6:2 FTS was degraded rapidly in the mixture with >90% removal achieved within 250 kGy. PFOS and PFNA (C8 compounds) showed good degradation with ~50% and ~ 60% degradation observed at 1000 kGy, respectively (Figure 12b). PFOA (C7) and PFHxS (C6) featured ~30% degradation at 250 kGy but did not undergo further degradation beyond that dose. PFOS and PFOA as individual contaminant achieved >90% degradation within 500 kGy. This experiment confirmed that there is competition between PFAS analytes for reaction with e_{aq}^- and reaction kinetics may vary with perfluorinated chain-length, the degree of fluorination in the carbon chain, functional group, and the presence of highly reactive intermediates. Complete degradation of 6:2 FTS (C6) compared to PFHpA (C6) suggests that polyfluorinated compounds are more reactive and undergo degradation easily compared to perfluorinated compounds. Similarly, degradation observed for PFHxS (C6) but not with PFHpA (C6) suggests that the reactivity is higher for sulfonate end group. These are speculative at this stage and more controlled experiments are needed to confirm the reactivity of PFAS compounds with e_{aq}^-.

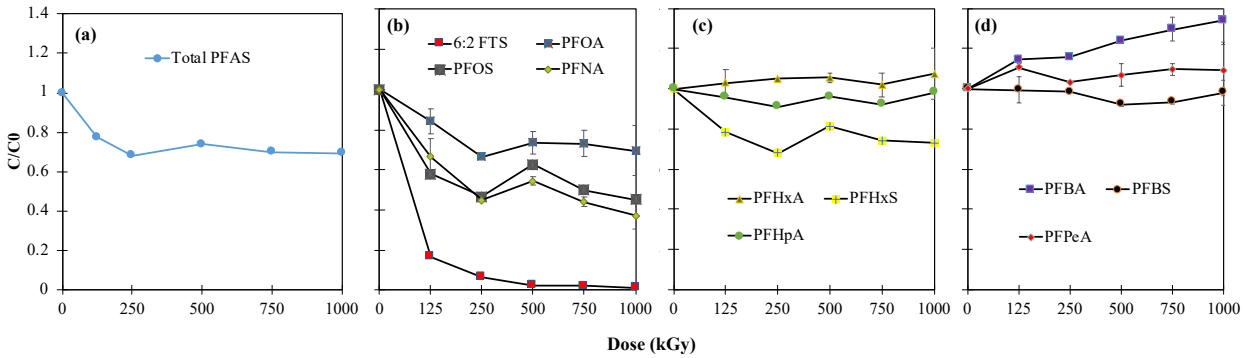

Figure 12. C/C_0 of total PFAS (a) and individual PFAS (b-d) of different chain lengths as a function of e-beam dose. Initial concentration of equimolar mixture of PFAS: 0.05 µM, DO: 2 mg/L.

PFHxA (C5), PFHpA (C6), and PFBS (C4) did not show any degradation during the experiment (Figures 12c-d). PFBA (C3) showed an increase in concentration by 34% at 1000 kGy. This can be attributed to the formation of short chain PFCAs as a result of degradation of long chain PFCAs such as PFOA and PFNA. However, the lack of degradation observed for the other PFAS is likely due to competition from long chain PFAS and the presence of highly reactive intermediates that may scavenge the available e_{aq}^-. We hypothesize that applying a higher dose (>1000 kGY) would lead to further removal of PFAS as we observed complete degradation of 100 ppb of individual PFAS within 500 kGy.

3.6. Treatment of contaminated groundwater samples using e-beam.

Three PFAS-contaminated groundwater samples (GW1, GW2, and GW3) were collected from two different US states to treat using optimized e-beam conditions. The goal for this experiment was to evaluate the effectiveness of e-beam to treat at environmentally relevant concentrations, compare the performance with controlled experiments (section 3.5.1), and observe the impacts of groundwater matrix. The total initial concentration of PFAS (ΣPFAS) was 18.8 ppb for GW1 (for 14 detected PFAS), 2.2 ppb for GW2 (for 10 detected PFAS), and 18.2 ppb for GW3 (for 17 detected PFAS). PFOS and PFHxS were the most abundant compounds in all three GW samples. The total removal of PFAS in GW1, GW2, and GW3 after a dose of 750 kGy was 36%, 71%, and 23% respectively (Fig 13a,b,c). The observed removal percentage for GW1 and GW3 was similar to the treatment of equimolar mixture PFAS in DIW. But unlike the treatment of equimolar mixture of PFAS in the previous section where the removal percentage was saturated after 250 kGy, we observed increasing removal tend from 250 to 750 kGy for GW1 and GW3. Hence, additional removal can be expected with increasing dose. However, the lack of complete removal of PFAS within 500 kGy in GW samples, which was observed for PFAS when treated individually in DIW, suggests the interference of GW matrix and the presence of competing co-contaminants (including other PFAS).

6:2FTS featured the highest removal (75 – 98%) in all three GW samples, followed by PFOS (25 – 80%), PFHxS (30 – 65%), and PFOA (15 – 54%) (Fig a1-2,b1-2,c1-2). These trends were similar to what was observed for the treatment of equimolar mixture of PFAS in DIW. Interestingly, we observed 95% removal of PFBA and 96% removal of PFBS from GW2. PFBS was also removed by 20% in GW1 and 74% in GW3 after 750 kGy. However, PFBA showed an

increase after treatment in GW1 and GW2 samples, similar to what was observed in the previous section for equimolar PFAS treatment. These differences are likely due to groundwater matrix interferences. GW2 featured low levels of PFAS compared to GW1 and GW3, that could have helped with the degradation of short chain PFBS and PFBA for two reasons: (i) the contribution of short chain PFAS after treatment of long chain PFAS was less, and/or (ii) relative competition to react with e_{aq}^- were low due to lower levels of PFAS in the sample.

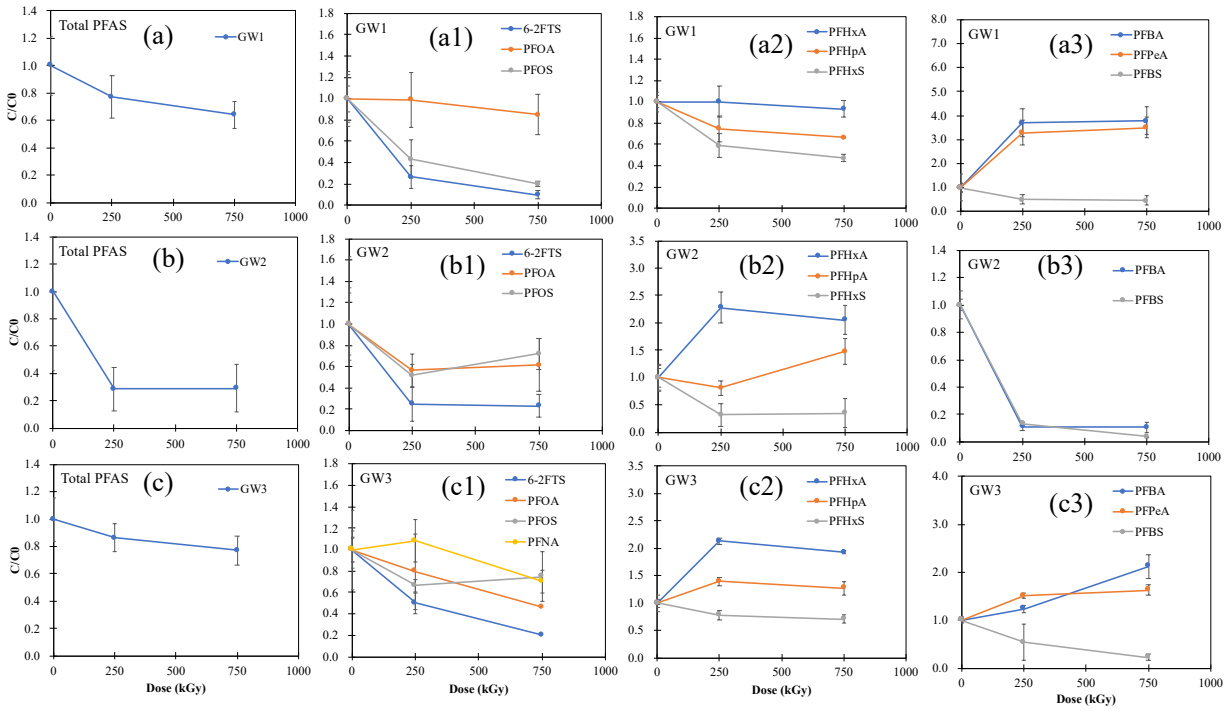

Figure 13. Degradation of PFAS in three contaminated groundwater samples collected from two different US states. Error bars represent minima and maxima from duplicate treatments.

3.7. Energy requirements and EEo calculations

Calculated EEo for the various contaminants treated in this study is summarized in Figure 14. As discussed already, 1,4-dioxane featured a low EEo and was comparable to other traditional AOP technologies. The EEo of various PFAS ranged from 48 to 1081 kWh/m^3/order, with 6:2FTS featuring the lowest value and PFBS featuring highest EEo value.

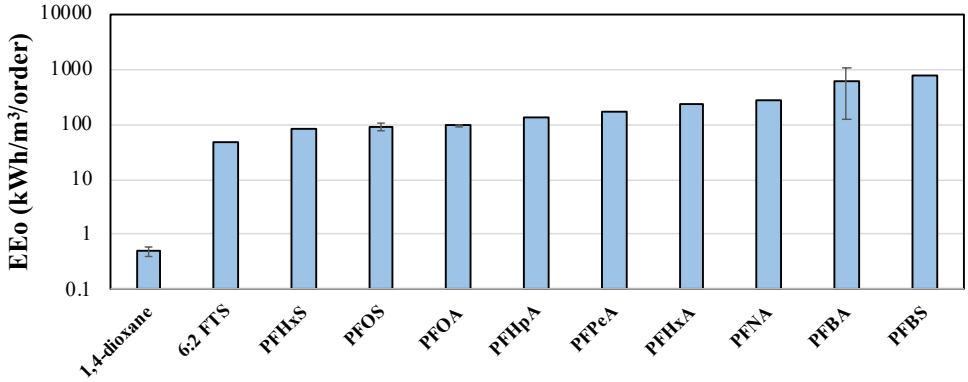

Figure 14. Calculated EEo for the treatment of 1,4-dioxane and PFAS using e-beam.

Figure 15 summarizes the range of EEo values reported for PFOA treatment by other destructive techniques and are compared with the calculated EEo values for e-beam treatment of PFOA. E-beam, when combined with the ideal water quality parameters (ideal DO and pH), gives a range of EEo values that are comparable and, in many cases, much lower than other destructive techniques such as activated persulfate and ultrasound, as well as electrochemical oxidation. This suggests that e-beam is a feasible technology from the point of energy consumption to decompose PFAS. The EEo values for e-beam can be enhanced by changing the initial PFAS concentration. On the basis of our discussion in section 3.4.3, it might be more favorable to use high initial concentrations of PFAS at an optimized dose in order to get energy efficient conditions for PFAS decomposition.

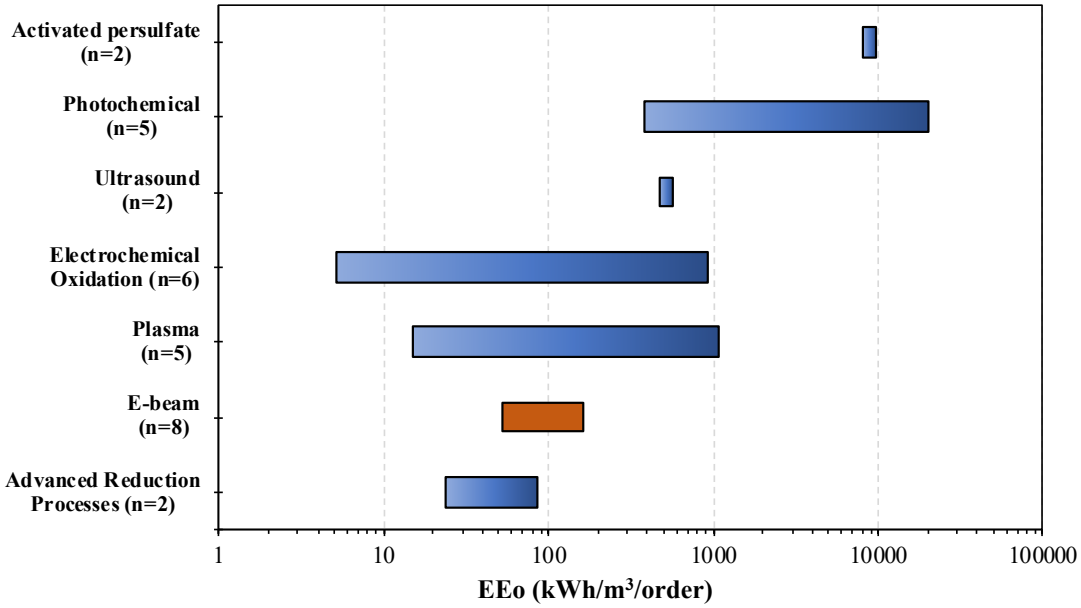

Figure 15. Calculated EEo of PFOA treatment by various destructive technologies.

4. CONCLUSIONS

This project has demonstrated that e-beam is highly effective in degrading 1,4-dioxane to below detection from an initial concentration ranging from 100 ppb to 1 ppm without the need for any sample modification at 5 kGy. The EEo values calculated from using e-beam technique are low comparable to traditionally used AOPs for 1,4-dioxane treatment like UV/hydrogen peroxide or ozone systems. One important advantage of using e-beam over other AOPs for 1,4-dioxane treatment is that it does not require any chemical additions. Traditional AOPs that rely on oxidants require careful dosing of chemicals in addition to planning for polishing filters to remove the excess/residual oxidants in the treated water.

E-beam technique has also shown great promise in the treating PFAS. The calculated EEo from this study are comparable to other destructive techniques, which make them a potential candidate to explore further. Treatment of PFAS-contaminated groundwater was similar to controlled DIW treatment of PFAS mixtures; however, complete removal was not observed due to interference of competing species present in the groundwater matrix. Results suggest improved degradation is feasible if higher doses (>1MGy) are applied to treat PFAS mixtures and real groundwater samples. Although we observed good removal of C4-C8 PFAS using e-beam, we

were unable to close the mass balance after treatment suggesting the presence of unknown transformation products.

Since the degradation of PFAS was similar for a wide range of initial concentrations, it is suggested from this work that the e-beam approach would be energy efficient when treating concentrated PFAS waste rather than directly treating drinking water. A combination of a pre-concentration step followed by e-beam irradiation (end-of-train treatment) would enable large-scale applications of e-beam treatment of PFAS. Shorter chain PFAS showed more resistance to degradation compared to long chain PFAS, suggesting more work is needed to understand the kinetics and reactivity of different PFAS as a function of chain length and functional group.

REFERENCES

1. Londhe, K., et al., Energy Evaluation of Electron Beam Treatment of Perfluoroalkyl Substances in Water: A Critical Review. *ACS ES&T Engineering* **2021**.
2. Rahman, M. F., et al., Behaviour and fate of perfluoroalkyl and polyfluoroalkyl substances (PFASs) in drinking water treatment: a review. *Water Res* **2014,** *50*, 318-40.
3. Buck, R. C., et al., Perfluoroalkyl and polyfluoroalkyl substances in the environment: terminology, classification, and origins. *Integr Environ Assess Manag* **2011,** *7*, (4), 513-41.
4. Kissa, E., *Fluorinated Surfactants and Repellents.* Marcel Dekker: New York, 2001.
5. Appleman, T. D., et al., Treatment of poly- and perfluoroalkyl substances in U.S. full-scale water treatment systems. *Water Res* **2014,** *51*, 246-55.
6. Nzeribe, B. N., et al., Physico-Chemical Processes for the Treatment of Per- And Polyfluoroalkyl Substances (PFAS): A review. *Crit Rev Environ Sci Technol* **2019,** *49*, (10), 866-915.
7. USEPA *Long-Chain Perfluorinated Chemicals (PFCs) Action Plan*; U.S. Environmental Protection Agency: 2009.
8. Vughs, D., et al., The determination of two emerging perfluoroalkyl substances and related halogenated sulfonic acids and their significance for the drinking water supply chain. *Environ Sci Process Impacts* **2019,** *21*, (11), 1899-1907.
9. Bjornsdotter, M. K., et al., Ultra-Short-Chain Perfluoroalkyl Acids Including Trifluoromethane Sulfonic Acid in Water Connected to Known and Suspected Point Sources in Sweden. *Environ Sci Technol* **2019,** *53*, 11093-11101.
10. Garnett, J., et al., Investigating the Uptake and Fate of Poly- and Perfluoroalkylated Substances (PFAS) in Sea Ice Using an Experimental Sea Ice Chamber. *Environ Sci Technol* **2021**.
11. Miner, K. R., et al., Deposition of PFAS 'forever chemicals' on Mt. Everest. *Sci Total Environ* **2020**, 144421.
12. Tian, S., et al., A 'Concentrate-&-Destroy' technology for enhanced removal and destruction of per- and polyfluoroalkyl substances in municipal landfill leachate. *Science of The Total Environment* **2021**.
13. The Third Unregulated Contaminant Monitoring Rule (UCMR 3): Data Summary, January 2017. https://www.epa.gov/dwucmr/third-unregulated-contaminant-monitoring-rule (November 2020),
14. Lee, C. S., et al., Impact of groundwater quality and associated byproduct formation during UV/hydrogen peroxide treatment of 1,4-dioxane. *Water Res* **2020,** *173*, 115534.
15. Adamson, D. T., et al., 1,4-Dioxane drinking water occurrence data from the third unregulated contaminant monitoring rule. *Sci Total Environ* **2017,** *596-597*, 236-245.
16. Matthew J. Zenker, R. C. B., and Morton A. Barlaz, Occurrence and Treatment of 1,4-Dioxane in aqueous environments. *Environmental Engineering Science* **2003,** *20*, (5).
17. Zhang, D. Q., et al., Adsorption of perfluoroalkyl and polyfluoroalkyl substances (PFASs) from aqueous solution - A review. *Sci Total Environ* **2019,** *694*, 133606.

18. Murray, C. C., et al., Removal of per- and polyfluoroalkyl substances using super-fine powder activated carbon and ceramic membrane filtration. *J Hazard Mater* **2019,** *366*, 160-168.
19. Kucharzyk, K. H., et al., Novel treatment technologies for PFAS compounds: A critical review. *J Environ Manage* **2017,** *204*, (Pt 2), 757-764.
20. Banks, D., et al., Selected advanced water treatment technologies for perfluoroalkyl and polyfluoroalkyl substances: A review. *Sep. Purif. Technol.* **2020,** *231*.
21. Mohr, T. K. G., et al., *Environmental investigation and remediation: 1,4-dioxane and other solvent stabilizers*. CRC Press, Taylor & Francis Group: Boca Raton, FL, 2010.
22. Getoff, N., Factors influencing the efficiency of radiation-induced degradation of water pollutants. *Radiation Physics and Chemistry* **2002**, (65), 437-446.
23. Kwon, M., et al., Removal of iopromide and degradation characteristics in electron beam irradiation process. *J Hazard Mater* **2012,** *227-228*, 126-34.
24. Song, Z., et al., Reductive defluorination of perfluorooctanoic acid by hydrated electrons in a sulfite-mediated UV photochemical system. *J Hazard Mater* **2013,** *262*, 332-8.
25. Bentel, M. J., et al., Defluorination of Per- and Polyfluoroalkyl Substances (PFASs) with Hydrated Electrons: Structural Dependence and Implications to PFAS Remediation and Management. *Environ Sci Technol* **2019,** *53*, (7), 3718-3728.
26. Trojanowicz, M., et al., Application of ionizing radiation in decomposition of perfluorooctanoate (PFOA) in waters. *Chem. Eng. J.* **2019,** *357*, 698-714.
27. Kim CG, S. H., Lee BR, Decomposition of 1,4-dioxane by advanced oxidation and biochemical process. *Journal of Environmental science and health,* **2006**, 599-611.
28. Kim, T. H., et al., Profiling the decomposition products of perfluorooctane sulfonate (PFOS) irradiated using an electron beam. *Sci Total Environ* **2018,** *631-632*, 1295-1303.
29. Trojanowicz, M., et al., Advanced Oxidation/Reduction Processes treatment for aqueous perfluorooctanoate (PFOA) and perfluorooctanesulfonate (PFOS) – A review of recent advances. *Chemical Engineering Journal* **2018,** *336*, 170-199.
30. Trojanowicz, M., et al., Application of ionizing radiation in decomposition of perfluorooctane sulfonate (PFOS) in aqueous solutions. *Chemical Engineering Journal* **2020,** *379*.
31. Ma, S.-H., et al., EB degradation of perfluorooctanoic acid and perfluorooctane sulfonate in aqueous solution. *Nuclear Science and Techniques* **2017,** *28*, (9), 137.
32. Wang, L., et al., Electron beam treatment for potable water reuse: Removal of bromate and perfluorooctanoic acid. *Chemical Engineering Journal* **2016,** *302*, 58-68.
33. Lee, C.-S., et al., Impact of groundwater quality and associated byproduct formation during UV/hydrogen peroxide treatment of 1,4-dioxane. *Water Res.* **2020,** *173*, 115534.
34. Stefan, M. I.; Bolton, J. R., Mechanism of the degradation of 1,4-dioxane in dilute aqueous solution using the UV/hydrogen peroxide process. *Environ. Sci. Technol.* **1998,** *32*, (11), 1588-1595.
35. Michael G. Nickelsen, W. J. C., David A. Secker, Louis A. Rosocha, Charles N. Kurucz, Thomas D. Waite, Kinetic modeling and simulation of PCE and TCE removal in aqueous solutions by electron-beam irradiation.pdf. *Radiat. Phys. Chem.* **2002,** *65*, 579-587.
36. Kim, T.-H., et al., Decomposition of perfluorooctane sulfonate (PFOS) using a hybrid process with electron beam and chemical oxidants. *Chem. Eng. J.* **2019,** *361*, 1363-1370.
37. Schulz, K., et al., Distribution and effects of branched versus linear isomers of PFOA, PFOS, and PFHxS: A review of recent literature. *Sci Total Environ* **2020,** *733*, 139186.
38. Gu, Y., et al., Efficient Reductive Decomposition of Perfluorooctanesulfonate in a High Photon Flux UV/Sulfite System. *Environ Sci Technol* **2016,** *50*, (19), 10554-10561.
39. Bentel, M. J., et al., Defluorination of per-and polyfluoroalkyl substances (PFASs) with hydrated electrons: structural dependence and implications to PFAS remediation and management. *Environ. Sci. Technol.* **2019,** *53*, (7), 3718-3728.

APPENDIX

Sample Analysis

For each sample batch, three samples were chosen at random to serve as analytical duplicates to account for accuracy of dilution and sample preparation. Similarly, three samples were randomly chosen and fortified with a known amount of PFAS analytes to account for the potential matrix effect and were termed as 'standard addition' samples. The method performance is shown in Table S1.

To account for the variability of the LC-MS/MS, isotopically labelled internal standards (1 ng each, Table S2) were added into each vial prior to the analysis. The detailed LC and MS conditions are listed in Table S3. Samples containing PFAS were scanned in the negative mode using the multiple reaction monitoring (MRM) function and the MRM transitions for each analyte are shown in Table S1. In general, each analyte has two MRM transitions (quantifier and qualifier) to confirm the robustness of the analysis. Data analysis was performed by Agilent MassHunter Quantitative Analysis B.09.00.

Samples containing 1,4-dioxane were extracted by liquid-liquid extraction. In brief, an 800 µL aliquot of the sample was transferred to a 2-mL centrifuge tube and spiked with surrogate (1,4-Dioxane-d_8). An equal volume of dichloromethane was added into the tube. The tubes were shaken vigorously for 2 minutes and then frozen at -80 ˚C for 30 min. The top frozen aqueous phase layer was discarded, and the bottom organic phase was collected for subsequent analysis by GC/MS. Prior to analysis, tetrahydrofuran-d_8 (THF-d_8) was added as an internal standard to monitor the instrumental stability throughout the analysis.

1,4-Dioxane was analyzed using an Agilent 7890/5975 gas chromatography mass spectrometer (GC/MS) with a fused silica capillary GC column (Agilent J&W CP-Select 624 CB, 30 m x 0.25 mm, 1.4 mm film thickness) connected to a mass spectrometer operated in selective ion monitoring (SIM) mode. Detailed instrument conditions are shown in Table S4. Data analysis was performed by Agilent ChemStation. For samples with high 1,4-Dioxane concentrations (e.g., 1000 ppm), the analysis was carried out by an Agilent 7890B GC equipped with a flame ionization detector (FID).

Aldehydes (formaldehyde, acetaldehyde, and glyoxal) were analyzed using the 2,4-dinitrophenylhydrazine (DNPH) derivatization method followed by HPLC-UV detection. Analysis of organic acids (formic, acetic, and oxalic acids) was performed using an ion chromatography.

Table S1. Analytical method performance

Batch#	Sample index	RPD* (%)	Sample index	Standard addition recovery (%)
5	5-1-a	0.3	5-1-a	86
	5-2-a	1.6	5-2-a	92
	5-3-a	3.0	5-3-a	97
6	6-1-a	2.3	6-1-a	109
	6-2-a	1.7	6-2-a	97
	6-3-a	0.4	6-3-a	127
7	7-1-a	2.0	7-1-a	85
	7-3-b	0.3	7-3-b	104
	7-7-a	2.9	7-7-a	85
8	8-1-a	2.5	8-1-a	96
	8-4-a-D	6.8	8-4-a-D	90
	8-5-b	0.2	-	-
9	9-1-a	3.2	9-1-a	151[#]
	9-5-a	0.2	9-5-a	58[#]
	9-5-d	1.0	9-5-d	99
10	10-1-a	7.0	10-1-a	97
	10-2-a	17.9	10-2-a	81
	10-4-b	1.3	10-4-b	80
	Average	3.0	Average	96
	stdev	4.2	stdev	20

*RPD = relative percentage difference of duplicate samples
[#]These samples were not used in interpretation of results

Table S2. MRM transitions for all compounds studied

Analyte	Full name	Internal standard	Precursor (m/z)	Product 1 (m/z)*	Product 2 (m/z)*
PFBA	Perfluorobutanoic acid	$^{13}C_4$-PFBA	213	169	-
PFPeA	Perfluoropentanoic acid	$^{13}C_5$-PFHxA	263	219	-
PFBS	Perfluorobutanesulfonic acid	$^{13}C_3$-PFBS	299	80	99
PFHxA	Perfluorohexanoic acid	$^{13}C_5$-PFHxA	313	269	119
PFHpA	Perfluoroheptanoic acid	$^{13}C_8$-PFOA	363	319	169
PFHxS	Perfluorohexanesulfonic acid	$^{13}C_3$-PFHxS	399	80	99
PFOA	Perfluorooctanoic acid	$^{13}C_8$-PFOA	413	369	169
6:2FTS	1H,1H, 2H, 2H-Perfluorooctane sulfonic acid	$^{13}C_8$-PFOS	427	407	81
PFNA	Perfluorononanoic acid	$^{13}C_8$-PFOA	463	419	169
PFOS	Perfluorooctanesulfonic acid	$^{13}C_8$-PFOS	499	80	99

*Products 1 and 2 serve as quantifier and qualifier, respectively.

Table S3. LC-MS/MS conditions

LC Instrument conditions	
Parameter	**Value**
LC	Agilent G7120A 1290 Binary Pump Agilent G7116A 1260 Multicolumn Thermostat Agilent G7167A 1260 Multisampler
Analytical column	Agilent ZOBRAX Eclipse Plus C18 3.0 x 50 mm, 1.8 micron
Delayed column	Agilent ZOBRAX Eclipse Plus C18 4.6 x 50 mm, 3.5 micron
Column temperature	50 °C
Injection volume	5 µL
Mobile phase	A) 5 mM Ammonium acetate in water B) Methanol
Flow rate	0.4 mL/min
Gradient	Time (min) %B
	0.0 10
	0.5 10
	2.0 30
	14.0 95
	14.5 100
Stop time	16.5 minutes
Post time	6 minutes
MS Instrument conditions	
Parameter	**Value**
MS	Agilent 6495 Triple Quadrupole MS/MS Agilent Jet Stream ESI source
Drying gas temperature	175 °C
Drying gas flow	17 L/min
Nebulizer	20 psi
Sheath gas temperature	275 °C
Sheath gas flow	11 L/min
Capillary voltage (Neg)	2500 V
Nozzle voltage (Neg)	0 V
iFunnel High pressure RF (Neg) Low pressure RF (Neg)	 90 V 40 V

Table S4. GC/MS conditions

Parameter	**Value**
Injection volume	1 µL, Spitless injection
Inlet temp	200 °C
Column	J&W CP-Select 624 CB (30 m x 0.25 mm, 1.4 µm film thickness)
Column Flow Rate	1 mL/min (Helium)
Column operation	30 °C (hold for 1 min) 90 °C (ramp at 7 °C/min) 200 °C (ramp at 20 °C/min, hold for 3 min)
Total run time	18 min
MS transfer line temp	150 °C
MS source temp	150 °C
MS quad temp	150 °C
Scan mode	**SIM**
THF	*d8*: m/z 46,78, and 80 (6 to 8 min)
1,4-Dioxane:	m/z 58, 88 (8 to 18 min)
1,4-Dioxane-*d8*	14.5 100
THF-*d8*:	m/z 46,78, and 80 (6 to 8 min)

Published manuscripts:

1. Londhe, K., Lee, C.S., Zhang, Y., Grdanovska, S., Kroc, T., Cooper, C., Venkatesan, A.K. (2021). Energy Evaluation of Electron Beam Treatment of Perfluoroalkyl Substances in Water: A Critical Review. *ACS ES&T Engineering*, 1(5), 827-841.

List of manuscripts planned for submission:

1. Efficient treatment of 1,4-dioxane-contaminated water using electron beam technology.
2. Treatment of short-chain and long-chain PFAS in groundwater using electron beam.